ν = kinematic viscosity, stokes
ζ = ratio of cross-sectional area of riser and downcomer, (−)
ρ = density, kg/m^3
σ = superficial tension, N/m
τ = shear stress, *Pa*
ϕ = hold-up, (−)
ϕ' = hold-up at z = 2.25 m, (−)

Indices

B = bottom
d = downcomer
F = friction
G = gas
H = hydrostatic
L = liquid
m = manometer
M = mixture
W = wall of the pipe
r = riser, relative

LITERATURE CITED

Bankoff, S. G., "A Variable Density Single-Fluid Model for Two-Phase Flow with Particular Reference to Steam-Water Flow," *J. Heat Transfer*, Trans. ASME, Series C., **82**, 265 (1960).

Belfield, A. R., Jr., "Experimental Studies of Oxygen Transfer in a Split Cylinder Air-Lift," M.S. Thesis, University of Maryland (1976).

Calderbank, P. H., M. B. Moo Young, and R. Bibby, *Third European Symposium on Chemical Reaction Engineering*, Pergamon Press (1964).

Freedman, W. and J. F. Davidson, "Hold-up and Liquid Circulation in Bubble Columns," *Trans. Inst. Chem. Eng.*, **47**, 251 (1969).

Gasner, L. L., "Development and Application of the Thin Channel Rectangular Air-Lift, Mass Transfer Reactor to Fermentation and Waste-Water Treatment Systems," *Biotechnol. Bioeng.*, **XVI**, 1179 (1974).

Gow, P. G., J. D. Littlehailes, S. R. L. Smith and R. B. Walter, "Single Cell Protein Production from Methanol: Bacteria," *Single Cell Protein II*, S. R. Tannenbaum and D. I. C. Wang, eds., Massachusetts Institute of Technology Press, Cambridge, Mass. (1975).

Hatch, R. T., "Experimental and Theoretical Studies of Oxygen Transfer in an Air-Lift Fermentor," Ph.D. Thesis, Massachusetts Institute of Technology (1973).

Hatch, R. T., and D. I. C. Wang, "Oxygen Transfer in the Air-Lift Fermentor," First Chemical Congress of the North American Continent, Mexico City (1975).

Hatch, R. T., A. G. Belfield and G. Goldhahn, "Oxygen Transfer in the Split-Cylinder Air-Lift," Annual Meeting of the American Chemical Society, Chicago, Ill. (1977).

Hells, J. H., "The Operation of a Bubble Column at High Throughputs, I. Gas Hold-up Measurements," *Chem. Eng. J.*, **12**, 89 (1976).

Ho, Ch. S., L. E. Erickson and L. T. Fan, "Modeling and Simulation of Oxygen Transfer in Air-Lift Fermentors," *Biotechnol. Bioeng.*, **XIX**, 1503 (1977).

Kanazawa, M., "The Production of Yeast from n-Parafins," *Single Cell Proteins II*, S. R. Tannenbaum and D. I. C. Wang, eds., Massachusetts Institute of Technology Press, Cambridge, Mass. (1975).

Kuraishi, M., N. Matsuda, A. Terao, K. Kamibayashi, K. Tonomura and T. Fujii, "A Study on the Internal Structure Design of Air-Lift Fermentors in the Production of Methanol Single Cell Protein," *Microbial Growth on C_1 Compounds*, Society of Fermentation Technology, Osaka, Japan, p. 231 (1975).

Le Francois, L., C. C. Mariller and J. V. Mejane, "Effectionnements aux Procedes de Cultures Forgiques et de Fermentations Industrielles," Brevet d'Invention, France, No. 1102200 (1955).

Legrys, G. A., "Power Demand and Mass Transfer Capability of Mechanically Agitated Gas-Liquid Contactors and their Relationship to Air-Lift Fermentors," *Chem. Eng. Sci.*, **33**, 83 (1977).

Marucci, G., "A Theory of Coalescence," *Chem. Eng. Sci.*, **23**, 975 (1969).

Merchuk, J. C., Y. Stein and R. I. Mateles, "A Distributed Parameter Model of an Air-Lift Fermentor," *Biotechnol. Bioeng.*, **22**, 123 (1980).

Nassos, G. P., and S. G. Bankoff, "Slip Velocity in an Air-Water System under Steady State and Transient Conditions," *Chem. Eng. Sci.*, **12**, 661 (1967).

Orazem, M. E., and L. E. Erickson, "Oxygen-Transfer Rates and Efficiencies in One and Two-Stage Air-Lift Towers," *Biotechnol. Bioeng.*, **XXI**, 69 (1979).

Schugerl, K., J. Lucko and U. Oels, "Bubble Column Bioreactors," *Adv. Biochem. Eng.*, **7**, 1 (1977).

Stein, Y., "Gas Hold-up, Liquid Circulation, and Mass Transfer Modeling and Simulation of a Tower Cycling Fermentor," MS Thesis, Ben Gurion University, Israel (1979).

Ueyama, K., and T. Miyauchi, "Behaviour of Bubbles and Liquid in a Bubble Column," *Kagaku Kogaku Rombunshu*, **3**, 19 (1977a).

Ueyama, K., and T. Miyauchi, "The Effects of Liquid Viscosity and Column Diameter on the Internal Circulating Flow in a Bubble Column," *Kagaku Kogaku Rombunshu*, **3**, 115 (1977b).

Wallis, G. B., "One-Dimensional Two-Phase Flow," McGraw Hill Inc., New York (1969).

Wang, D. I. C., "Proteins from Petroleum," *Chem. Eng.*, **75**, 99 (1968).

Zuber, R. N., and J. A. Findley, "Average Volumetric Concentrations in Two-Phase Flow Systems," *J. Heat Transfer*, **87**, 453 (1965).

Manuscript received July 13, 1979; revision received June 15, and accepted June 27, 1980.

Pressure Fluctuations in a Fluidized Bed

An on-line statistical study of the pressure fluctuations in fluidized beds was conducted by using pressure transducers, a correlation and probability analyzer and a Fourier transform analyzer. The causes of the fluctuations were explored, and the effects of the gas velocity, bed height, particle size and distributor design on the major frequency and amplitude of the fluctuations were investigated. The results indicate that the motion of bubbles appears to be the major cause of the pressure fluctuations in the upper portion of a fluidized bed. In the lower portion, the combined effects of the formation of large bubbles in the middle portion of the bed, the formation of small bubbles near the distributor, and the jet flow immediately above the distributor appear to be the major causes of pressure fluctuations.

L. T. FAN
THO-CHING HO
S. HIRAOKA
and
W. P. WALAWENDER

Department of Chemical Engineering
Kansas State University
Manhattan, Kansas 66506

SCOPE

Pressure fluctuations have been observed to occur in most fluidized beds and these fluctuations have been used to define an index for the quality of fluidization (Shuster and Kisliak, 1952; Fiocco, 1964; Sutherland, 1964; Winter, 1968). Small and rapid fluctuations are considered to be associated with a good quality of fluidization.

The nature of pressure fluctuations in a fluidized bed is a complex function of particle properties, bed geometry, pressure in the bed, and properties and flow conditions of the fluidizing fluid. The pressure fluctuations have been studied by

0001-1541-81-3078-0388-$2.00.

several investigators (Tamarin, 1964; Swinehart, 1966; Hiby, 1967; Kang et al., 1967; Lirag and Littman, 1971; Wong and Baird, 1971; Verloop and Heertjes, 1974). However, the phenomena of pressure fluctuations have not yet been fully understood because of their complexity and the limitation in the available techniques and facilities for measuring them.

The previous investigations have led to two different conclusions about the cause of pressure fluctuations in a fluidized bed. Tamarin (1964) and Hiby (1967) have concluded that the pressure fluctuations are related to the passage of bubbles through the upper boundary of the bed and to the changes in the height of the bed. Lirag and Littman (1971) have also concluded that the bed height fluctuations, resulting from bubbles escaping at the surface of the bed, cause the pressure fluctuations. Kang et al. (1967), however, have concluded that the action of bubbles causes changes in the mode and condition of gas flow and porosity in the dense phase, and eventually induces the pressure fluctuations.

Among the investigators, Swinehart (1966), Kang et al. (1967) and Lirag and Littman (1971) used statistical approaches. Swinehart (1966) calculated the cross-correlation function between two pressure fluctuation signals taken from two vertically separated pressure taps and determined the "correlation-average propagation velocity" of bubbles in a fluidized bed. Kang et al. (1967) and Lirag and Littman (1971) calculated the probability density function, the autocorrelation function, and the power spectral density function of the pressure fluctuations off-line. The resultant autocorrelation function and power spectral density function were then used to determine the frequency and the root mean square of the fluctuations. Lirag and Littman (1971) also used the measured frequency to estimate the bubble size. The above investigators have amply demonstrated the power of the statistical analysis or correlation approach in analyzing the random pressure fluctuation signals in a fluidized bed; however, excessive time and effort needed to employ it off-line have prevented its wide-spread uses in systematic studies of fluctuation phenomena in process systems.

In this work, an on-line approach was used to statistically analyze the pressure fluctuations in a fluidized bed. The probabilistic and statistical characteristics of the pressure fluctuations along the fluidized bed including the jet zone adjacent to the distributor plate were studied. The causes of the fluctuations were explored, and the effects of the gas velocity, bed height, particle size and distributor design on the major frequency and amplitude of the fluctuations were investigated. The measured major frequencies were compared with the results predicted from the model proposed by Verloop and Heertjes (1974).

CONCLUSIONS AND SIGNIFICANCE

A study of the pressure fluctuations in a fluidized bed with on-line measurement and data processing has been found to be efficient with respect to computational effort and to give sufficiently accurate results from the statistical point of view. The study has given rise to the following conclusions:

1. The motion of bubbles causes pressure fluctuations in the upper portion of a fluidized bed. The major pressure fluctuations in the lower portion of the bed are caused by the formation of large bubbles in the middle of the bed through bubble coalescence. However, the small pressure fluctuations, which are superimposed on the major fluctuations in the lower half of the pressure-time curve, are caused by the formation of small bubbles near the distributor and the jet flow right above the distributor.

2. The static bed height has a significant effect on the major frequency of the pressure fluctuations, whereas the air flow rate, the distributor design, and the particle size do not significantly affect the major frequency. The measured major frequencies are in fairly good agreement with the results predicted from the equation derived by Verloop and Heertjes (1974).

3. The amplitude of the pressure fluctuations is related to both the bed density and the size of bubbles which are the sources of the pressure fluctuations.

4. The probability density profile of a pressure fluctuation signal around its mean has different shapes at different locations of the bed. It skews to the negative side at the bottom of the bed, is nearly symmetrical at the middle, and skews to the positive side at the top of the bed.

Pressure fluctuation signals can be employed for calculating bubble size (Lirag and Littman, 1971) and measuring bubble rise velocity (Swinehart, 1966). The analysis of pressure fluctuations for determining their density function, frequency, and power spectral density function could also be a useful way of monitoring changes in bed conditions and for diagnosing abnormalities in bed operation. Pressure fluctuations in a fluidized bed can enhance vibrations of heater tubes in a fluidized bed combustor or boiler; thus, this analysis is essential for reliable design of such a system.

THEORETICAL

For a continuous stationary random variable $X(t)$, its probability density function $f_{X(t)}(x)$ can be calculated as:

$$f_{X(t)}(x)\Delta x \equiv \lim_{T\to\infty} \frac{1}{T} \Sigma(\Delta T) \tag{1}$$

The probability distribution function is a cumulative function of the probability density function, i.e.,

$$F_{X(t)}(x) \equiv \int_{-\infty}^{x} f_{X(t)}(x)dx \tag{2}$$

The first moment of $X(t)$, i.e., the mean, is defined as:

$$\mu \equiv \int_{-\infty}^{\infty} x f_{X(t)}(x)dx \tag{3}$$

The r-th central moment of $X(t)$ about its mean, μ_r, is defined as:

$$\mu_r \equiv E[(x(t) - \mu)^r] = \int_{-\infty}^{\infty} (x - \mu)^r f_{X(t)}(x)dx \tag{4}$$

Note that the first central moment is equal to zero, and the second central moment is the variance of $X(t)$. The nondimensionalized third central moment, defined as:

$$S \equiv \frac{\mu_3}{\sigma^3} = \frac{1}{\sigma^3} \int_{-\infty}^{\infty} (x - \mu)^3 f_{X(t)}(x)dx \tag{5}$$

is the skewness, which is a measure of the lack of symmetry in $f_{X(t)}(x)$ about the mean. The nondimensionalized fourth central moment, defined as:

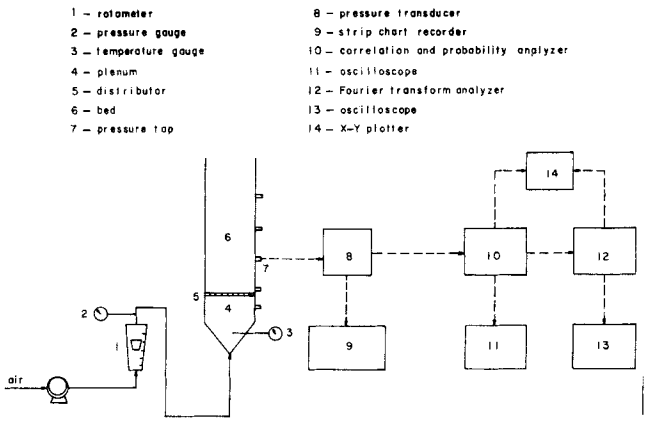

Figure 1. Experimental facilities.

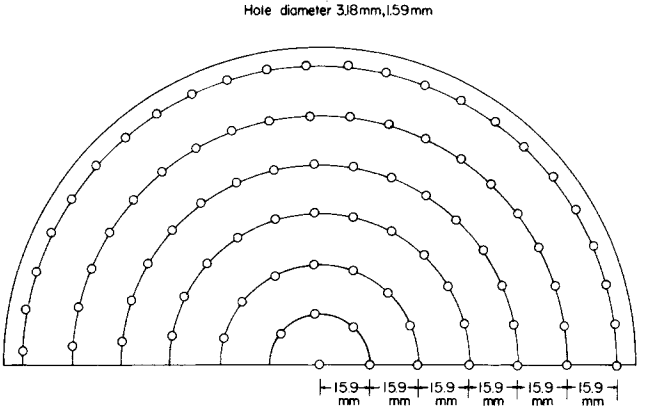

Figure 2. Hole layout of distributor.

$$K \equiv \frac{\mu_4}{\sigma^4} = \frac{1}{\sigma^4}\int_{-\infty}^{\infty}(x-\mu)^4 f_{X(t)}(x)dx \tag{6}$$

is the kurtosis or flatness factor, which is a measure of the extent of the skirt of $f_{X(t)}(x)$ about the mean.

Under the assumption of ergodicity, the mean and the variance can also be expressed, respectively, as:

$$\mu = \lim_{T\to\infty}\frac{1}{T}\int_{-\frac{T}{2}}^{\frac{T}{2}} x(t)dt \tag{7}$$

and

$$\sigma^2 = \lim_{T\to\infty}\frac{1}{T}\int_{-\frac{T}{2}}^{\frac{T}{2}}(x(t)-\mu)^2 dt \tag{8}$$

And, the auto-correlation and the cross-correlation can be expressed, respectively, as:

$$\phi_{xx}(\tau) = \lim_{T\to\infty}\frac{1}{T}\int_{-\frac{T}{2}}^{\frac{T}{2}} x(t)x(t+\tau)dt \tag{9}$$

and

$$\phi_{xy}(\tau) = \lim_{T\to\infty}\frac{1}{T}\int_{-\frac{T}{2}}^{\frac{T}{2}} x(t)y(t+\tau)dt \tag{10}$$

Note that if $X(t)$ has a zero mean, $\phi_{xx}(0)$ defines the variance of $X(t)$.

The power spectral density function $S_{xx}(\omega)$ of $X(t)$ is the Fourier transform of its auto-correlation function, i.e.,

$$S_{xx}(\omega) = \int_{-\infty}^{\infty}\phi_{xx}(\tau)e^{-j\omega t}d\tau \tag{11}$$

The function expresses the behavior of a signal in the frequency domain rather than in the time domain. For details of the statistical analysis of random functions, the reader is referred to treaties by Bendat(1958), Brown and Nilsson(1962), Crandall and Mark(1963), Davenport and Root(1958), and Lee(1960).

Verloop and Heertjes (1974) have derived an expression, which relates the major frequency of pressure fluctuations to the bed height as:

$$f = \frac{1}{2\pi}\sqrt{\frac{g}{L}\left(\frac{2-\epsilon}{\epsilon}\right)} \tag{12}$$

In deriving this expression, they have assumed that all particles move in phase and have the same frequency, and that the fluid moves in phase with the particles. Furthermore, they have considered that the fluid velocity with respect to the particles, instead of the superficial velocity, is constant.

TABLE 1. PHSYSICAL PROPERTIES OF SAND AND TEST RANGE OF EXPERIMENTAL VARIABLES.

Experimental Variables	Test Range
Sand Size	Sieve No. 20-30 $\bar{D}_p$ = 0.000711 m; ρ_{mf} = 2640 kg/m^3; ϵ_{mf} = 0.46; U_{mf} = 0.368 m/s
	Sieve No. 30-40 $\bar{D}_p$ = 0.000491 m; ρ_{mf} = 2620 kg/m^3; ϵ_{mf} = 0.47; U_{mf} = 0.140 m/s
Distributor	Two: hole diameter 0.00316 m & 0.00158 m
U/U_{mf}	1.25-2.50
Static Bed Height	0.04 m-0.50 m

EXPERIMENTAL

The facilities and prodedure employed in carrying out experiments and measurements are described in this section.

Facilities

A schematic diagram of the experimental facilities is shown in Figure 1. The fluidized bed assembly included a bed column, a distributor and a plenum column. The bed and plenum columns, which were fabricated from "plexiglass" to permit visual observation, were 0.203 m(8 in.) in diameter and were 3 m and 0.17 m long, respectively. The two distributors used were perforated aluminum plates, 0.00158 m (1/16 in.) thick and had 164 holes. The holes in one of the plates had a diameter of 0.00316 m (1/8 in.) and the other a diameter of 0.00158 m (1/16 in.). The layout of holes in the distributors is shown in Figure 2. The pressure drop ratio ($\Delta P_{ll}/\Delta P_{bed}$) for the distributor with the hole diameter of 0.00316 m was about 10-15% and that for the distributor with the hole diameter of 0.00158 m was about 20-40% for most of the experimental runs. Two types of sand were used as the fluidizing particles. Their physical properties and the experimental conditions are summarized in Table 1.

Pressure taps were installed vertically along the columns. The distance between two adjacent taps was about 0.045 m. The inside opening of each tap was covered with a screen to prevent the sand from entering the tap. The outside opening of a tap was connected to a differential pressure transducer (Enterprise Model CD3J), which had two input channels and produced an output voltage proportional to the pressure difference between the two input channels. In measuring the pressure fluctuations at a specific location (tap), the tap was connected to the positive input channel while the other channel was left exposed to the atmosphere. With the use of interchangeable diaphrams, the transducer provided a multirange working capacity. Two transducers, each with a diaphram capacity of ±6.89 kPa (±1 psi), were used. The lines which connected the taps and the transducers were balanced so that constant transient response could be maintained.

The calculating and recording assembly included a correlation and probability analyzer (Honeywell Model SAI-43A), a Fourier trans-

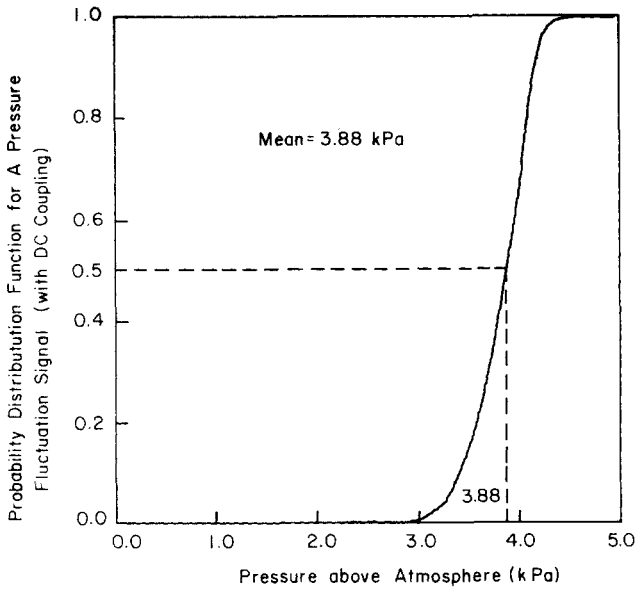

Figure 3. Sample calculation of the mean of a pressure fluctuation signal.

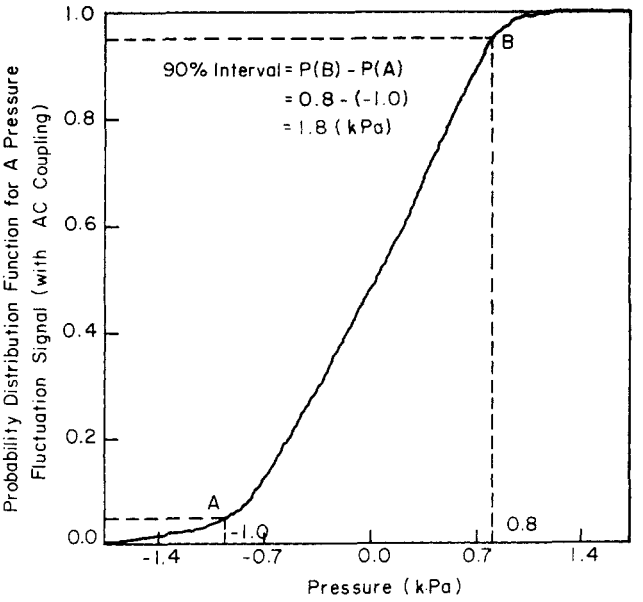

Figure 4. Sample calculation of the 90% fluctuation interval.

form analyzer (Honeywell Model SAI-470), a strip chart recorder, an *X-Y* plotter, and two oscilloscopes. The correlation and probability analyzer executed calculations of the auto-correlation function, the cross-correlation function, the probability density function, and the probability distribution function of a fluctuation signal. The analyzer had two input channels, each had selection buttons AC and DC. The sampling interval of the analyzer ranged from 2 μs to 1 s, while the total number of sampling points in a calculation could be up to 128 × 1024. The Fourier transform analyzer transformed the auto-correlation function in the time domain into the corresponding power spectral density function in the frequency domain according to Eq. 11. The calculated or transformed functions were either directly exhibited on an oscilloscope or recorded on an *X-Y* plotter.

Measurement

For each run at a specific combination of experimental variables, pressure fluctuations at each selected location (tap) along the bed and plenum columns were detected by connecting the tap to a pressure transducer. The voltage-time (corresponding to pressure-time) signal from the transducer was sent to both the strip chart recorder and the correlation and probability analyzer. The recorder registered the pressure-time signal, and the calculating assembly computed the auto-correlation function, the probability density function, the probability distribution function and the power spectral density function of the pressure fluctuation signal. The sampling interval for calculating the auto-correlation, density, and distribution functions was selected to be 10 ms, and a total of 8 × 1024 points were sampled or measured. This gave rise to an operating time of 80 s.

The properties of a pressure fluctuation signal measured were its mean, major frequency, average amplitude, root mean square, 90% fluctuating interval and probability density profile. The probability distribution function, calculated using DC coupling, was employed to determine the mean of the fluctuation signal. It was accomplished by reading the *X*-axis value of the $F_{X(t)}$ (0.5) point, as shown in Figure 3.

The major frequency of a fluctuation signal was determined from locating the peak of its power spectral density function. The on-line measurement was carried out on an oscilloscope with the help of a bin marker. The root mean square of a pressure fluctuation signal was obtained by calculating the square root of the value at zero time shift of its auto-correlation function.

The pressure-time curve registered on the strip chart recorder was used to calculate the average amplitude of a pressure fluctuation signal. It was determined by averaging the individual amplitudes along a chart distance equivalent to 8 s. In the calculation, it was necessary to take into account only those amplitudes corresponding to the frequencies near the major frequency.

The probability distribution function, which was calculated employing AC coupling, was used to determine the 90% fluctuating interval of a pressure fluctuation signal. A sample calculation is shown in Figure 4. The fluctuating range between points A and B in the figure stands for its 90% fluctuating interval. The probability density function of a pressure fluctuation signal was calculated by the correlation and probability analyzer as mentioned previously. The function itself showed the characteristic properties of the pressure fluctuations.

The cross-correlation function between two fluctuation signals which were taken simultaneously at two locations (taps) by the two transducers was also calculated by the correlation and probability analyzer. Sampling interval ranged from 0.1 to 1 ms and the total sampling points from 64 × 1024 to 128 × 1024. The on-line measurements of the time shift between the two fluctuations were made on an oscilloscope with the help of a bin marker.

RESULTS AND DISCUSSION

Pressure fluctuation signals were registered on the strip chart recorder. The typical pressure-time curves are shown in Figures 5 and 6. The typical probability density function, auto-correlation function, and power spectral density function re-

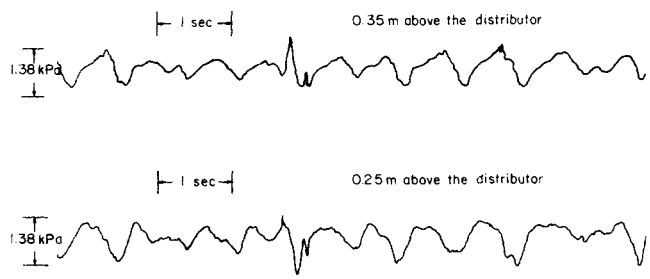

Figure 5. Pressure fluctuation signals detected simultaneously from two pressure taps in the upper portion of a deep fluidized bed ($\bar{D}_p$ = 0.000711 m, L_s = 0.4 m, U/U_{mf} = 1.5).

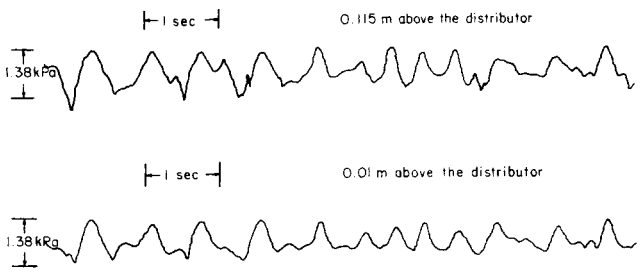

Figure 6. Pressure fluctuation signals detected simultaneously from two pressure taps in the lower portion of a deep fluidized bed ($\bar{D}_p$ = 0.000711 m, L_s = 0.4 m, U/U_{mf} = 1.5).

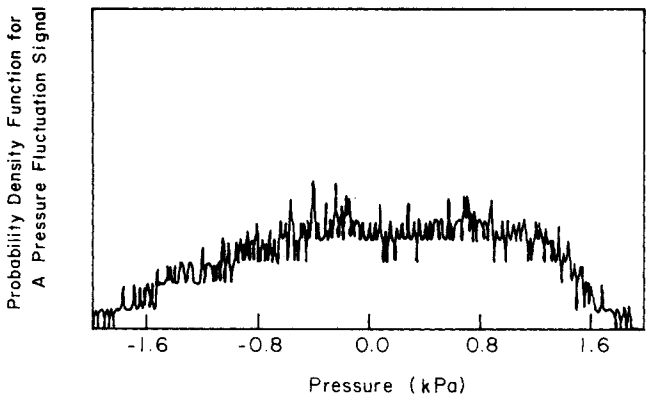

Figure 7. Probability density function of a pressure fluctuation signal ($\bar{D}_p$ = 0.000711 m, L_s = 0.35 m, U/U_{mf} = 2.0, probe location: 0.2 m above the distributor).

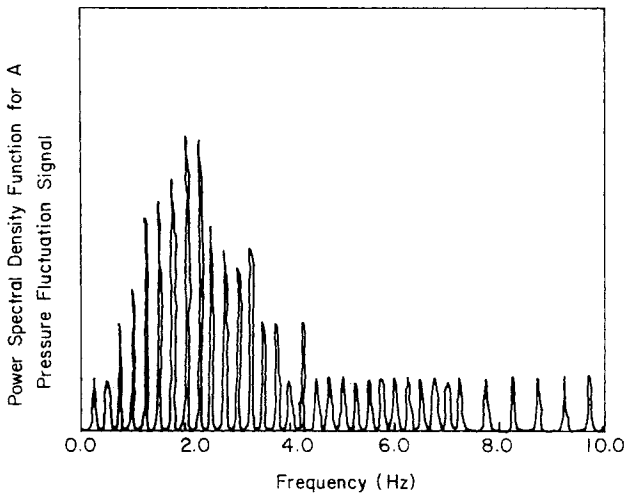

Figure 9. Power spectral density function of a pressure fluctuation signal ($\bar{D}_p$ = 0.000711 m, L_s = 0.35 m, U/U_{mf} = 2.0, probe location: 0.2 m above the distributor).

corded are shown in Figures 7, 8, and 9, respectively. The experimental results for static bed heights 0.06 m and 0.10 m are summarized in Table 2, and those for 0.40 m in Table 3. The effect of static bed height on the major frequency is shown in Figure 10.

The probability density functions recorded at different axial positions along the fluidized bed under the same set of experimental conditions are shown in Figure 11. The figure also shows their mean, variance, skewness and kurtosis. In Figure 12, the mean pressure and the 90% interval of the pressure fluctuations

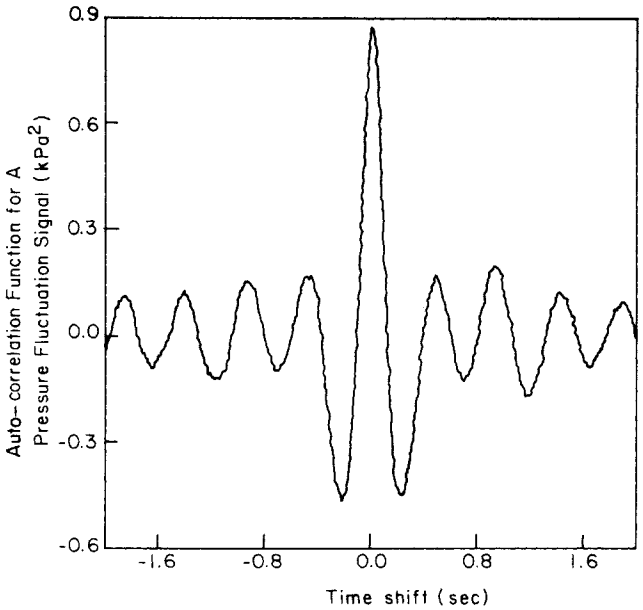

Fugure 8. Auto-correlation function of a pressure fluctuation signal ($\bar{D}_p$ = 0.000711 m, L_s = 0.35 m, U/U_{mf} = 2.0, probe location: 0.2 m above the distributor).

at a specific location in a fluidized bed are plotted against the air flow rate for one set of experimental conditions.

Periodicity of Pressure Fluctuations

The presence of a periodic component in the pressure fluctuations in fluidized beds was identified by Lirag and Littman (1971) from analyzing the recorded probability density function, auto-correlation function and power spectral density function of the pressure fluctuations. The same functions obtained in this work confirmed the existence of periodic phenomena. Specifically, it has been observed that the probability density function has a saddle shape about the mean, the auto-correlation function has a sinusoidal shape, and the power spectral density function exhibits a sharp peak. These observations are illustrated in Figures 7, 8, and 9.

Cause of Pressure Fluctuations

The cause of pressure fluctuations in the upper portion of a deep fluidized bed is discussed first. Here, the deep fluidized bed refers to the fluidized bed with a static bed height greater than 0.25 m ($L_s/D_t \geq 1.25$), and the upper portion refers to the portion of the bed where only one bubble at a time was observed to pass the horizontal plane.

TABLE 2. EXPERIMENTAL RESULTS WITH LOW STATIC BED HEIGHTS.

Distributor*	$\bar{D}_p$ (m)	L_s (m)	Fluctuation**	U/U_{mf} 1.25	1.50	1.75	2.00
A	0.000711	0.06	Fre (Hz)	5.00	4.75	4.75	4.75
			Amp (kPa)	0.10	0.14	0.16	0.19
		0.10	Fre (Hz)	3.50	3.50	3.25	3.25
			Amp (kPa)	0.13	0.19	0.24	0.38
B	0.000711	0.06	Fre (Hz)	5.25	5.25	5.00	5.00
			Amp (kPa)	0.06	0.09	0.12	0.16
		0.10	Fre (Hz)	3.75	3.75	3.50	3.50
			Amp (kPa)	0.10	0.16	0.20	0.35
A	0.000491	0.06	Fre (Hz)	5.00	5.00	5.50	5.50
			Amp (kPa)	0.05	0.06	0.07	0.12
		0.10	Fre (Hz)	3.00	3.50	3.50	4.00
			Amp (kPa)	0.07	0.14	0.16	0.19

*Distributor: A—hole diameter 0.00316 m; B—hole diameter 0.00158 m.
**Fluctuation: FRE—major frequency; Amp—amplitude.

TABLE 3. EXPERIMENTAL RESULTS WITH 0.4 M STATIC BED HEIGHT.

Distributor*	$\bar{D}_p$ (m)	U/U_{mf}	Fluctuation**	Probe Location (Distance above Distributor, m) plenum	0.01	0.055	0.105	0.150	0.195	0.230	0.285
A	0.000711	1.25	Fre (Hz)	1.25	1.25	1.25	1.25	1.50	1.50	1.25	1.25
			Amp (kPa)	0.31	0.31	0.31	0.35	0.35	0.38	0.38	0.38
		1.50	Fre (Hz)	1.75	1.75	1.75	1.50	1.50	1.75	1.50	1.75
			Amp (kPa)	0.64	0.60	0.60	0.64	0.66	0.70	0.73	0.66
		2.00	Fre (Hz)	1.50	1.50	1.50	1.50	1.50	1.50	1.50	1.50
			Amp (kPa)	1.95	1.90	1.90	2.00	2.07	2.14	1.90	1.45
B	0.000711	1.25	Fre (Hz)	1.00	1.00	1.00	1.25	1.25	1.25	1.25	1.50
			Amp (kPa)	0.10	0.12	0.15	0.19	0.24	0.28	0.28	0.28
		1.50	Fre (Hz)	1.50	1.50	1.50	1.50	1.50	1.50	1.50	1.50
			Amp (kPa)	0.31	0.41	0.41	0.48	0.52	0.59	0.66	0.66
		2.00	Fre (Hz)	1.50	1.50	1.50	1.50	1.50	1.50	1.50	1.50
			Amp (kPa)	1.17	1.31	1.32	1.45	1.50	1.59	1.56	1.38
A	0.000491	1.25	Fre (Hz)		1.25			1.25		1.75	1.50
			Amp (kPa)		0.13			0.21		0.48	0.48
		1.50	Fre (Hz)		1.50			1.50		1.75	1.75
			Amp (kPa)		0.34			0.52		0.55	0.48
		2.00	Fre (Hz)		1.75			1.75		2.00	2.50
			Amp (kPa)		0.69			0.83		0.83	0.69

* Distributor: A—hole diameter 0.00316 m; B—hole diameter 0.00158 m.
** Fluctuation: Fre—major frequency; Amp—amplitude.

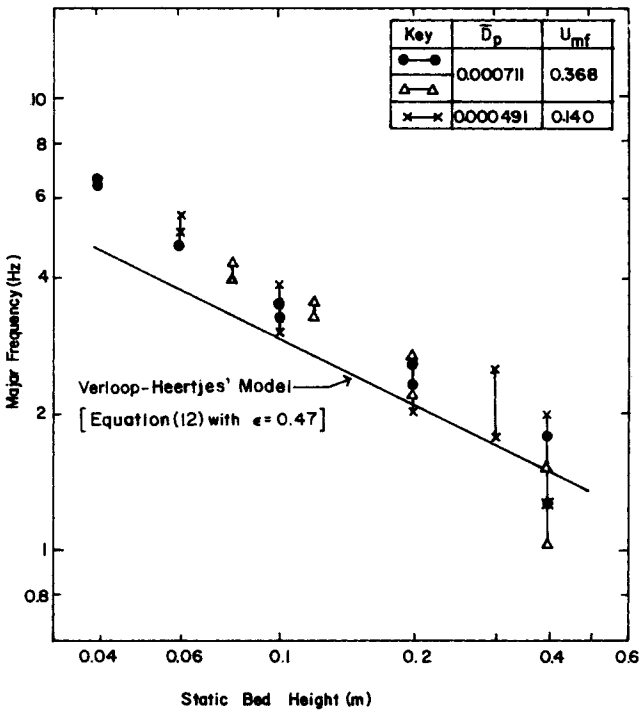

Figure 10. Effect of static bed height on the major frequency.

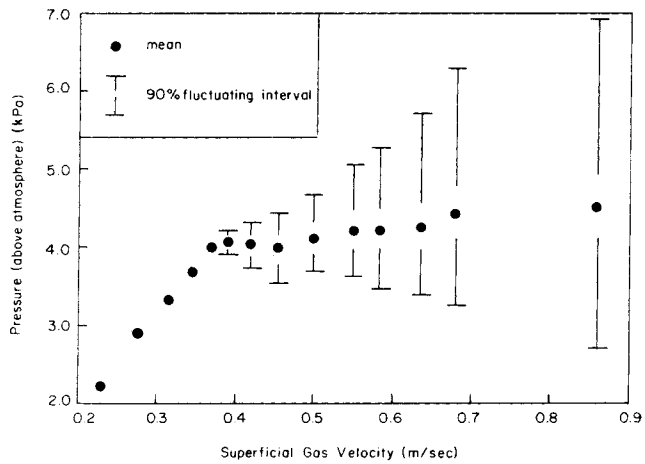

Figure 12. Pressure vs. velocity curve in a fluidized bed at 0.15 m above the distributor ($\bar{D}_p$ = 0.000711 m, L_s = 0.4).

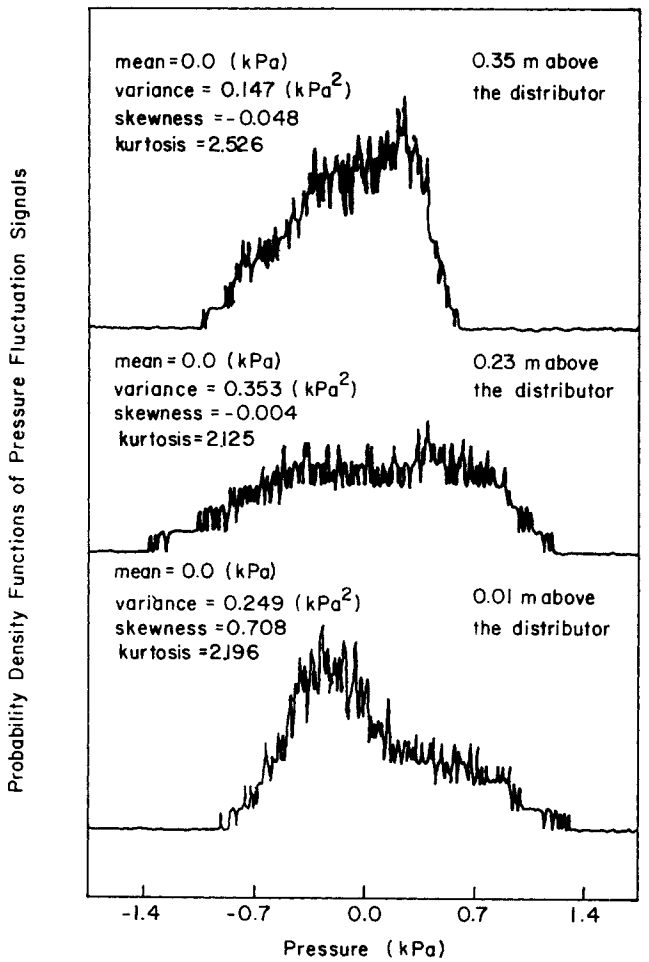

Figure 11. Probability density functions at different locations of a fluidized bed ($\bar{D}_p$ = 0.000711 m, L_s = 0.4 m, U/U_{mf} = 1.75).

Figure 5 shows portions of two typical pressure fluctuation signals detected simultaneously from two pressure taps which were vertically apart. In the figure, the upper and lower curves correspond to the pressure fluctuations in the bed at 0.35 m and 0.25 m above the distributor, respectively. A comparison of the two curves indicates that the major fluctuating frequency for both curves is the same. However, the upper curve shows a slight time delay from the lower curve. The magnitude of delay was measured from the cross-correlation function between the

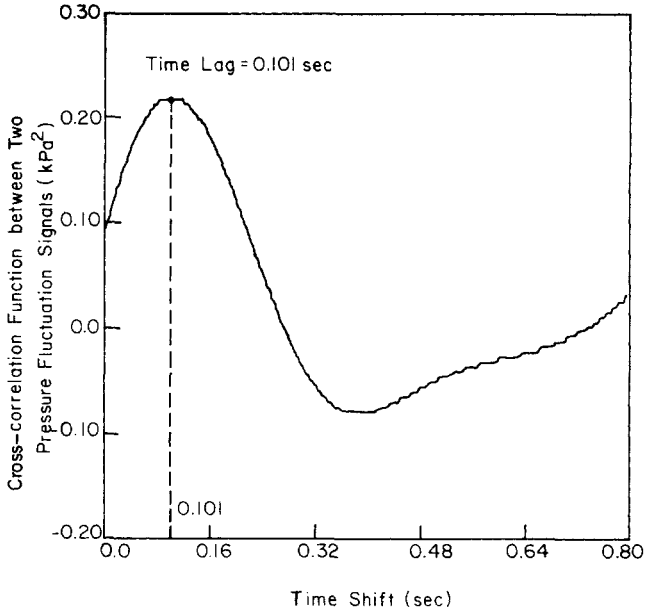

Figure 13. Cross-correlation function between two pressure fluctuation signals ($\overline{D}_p$ = 0.000711 m, L_s = 0.4 m, U/U_{mf} = 1.5).

two pressure fluctuation signals. The resultant cross-correlation function is shown in Figure 13. The figure indicates that the signal from the upper tap has a time delay of 0.101 s compared to the signal from the lower tap. This value agrees approximately with that estimated from the two curves in Figure 5. Similar observations were made under other experimental conditions.

If the pressure fluctuations were caused by the bed height fluctuations as concluded by Lirag and Littman (1971), the pressure fluctuation signal at the upper position should occur in advance. Since this was not the case, we would say that the pressure fluctuations in the upper portion of a deep fluidized bed are not directly caused by the bed height fluctuations.

To interpret the observed results meaningfully, the pressure-time curve for a single rising bubble in a fluidized bed was examined. Figure 14 shows a pressure-time curve during the rise of a single injected bubble as presented by Littman and Homolka (1970). In their study, the bubble was injected into an incipiently fluidized bed below a pressure tap, and a pressure transducer was used to detect the pressure changes at the tap during the rise of the bubble. Using a photographic method, they found that point 3 of the curve in the figure corresponded to the instant when the roof of the bubble reached the tap, and point 5 corresponded to the instant when the floor of the bubble reached the pressure tap. Therefore, the figure shows that the motion of a bubble in a fluidized bed tends to produce a pressure change at every position.

A comparison of the pressure-time curve of a single rising bubble (Figure 14) with each fluctuating cycle of the pressure fluctuation curve (Figure 5) indicates the pressure fluctuation curve could be the result of serially connecting the partially overlapping pressure-time curves of successive rising bubbles. The observation that only one bubble at a time passed the pressure tap confirms the fact that the continuous upward motion of bubbles causes the pressure fluctuations in the upper

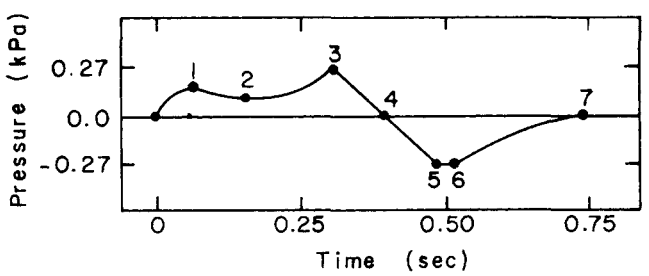

Figure 14. Pressure-time curve during the rise of a bubble (Littman and Homolka, 1970).

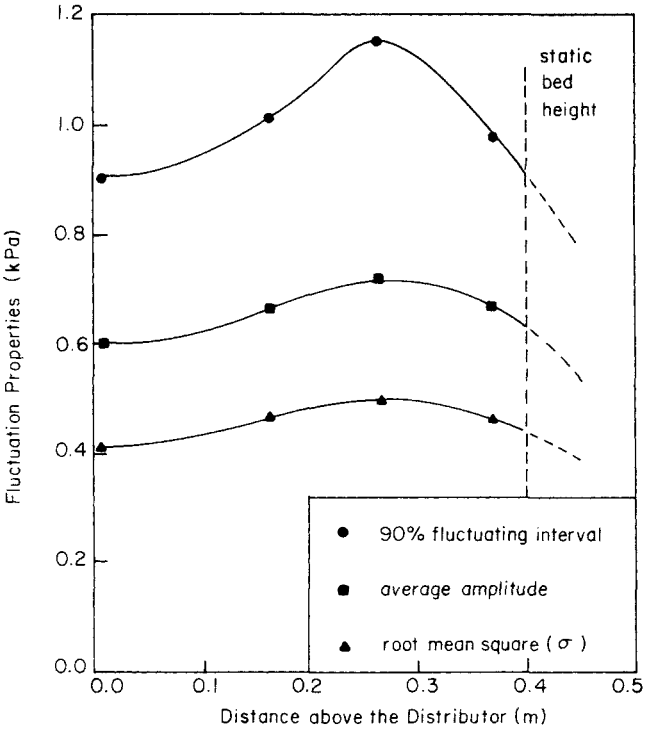

Figure 15. Values of 90% fluctuating interval, average amplitude and root mean square of pressure fluctuation signals along the bed column ($\overline{D}_p$ = 0.000711 m, L_s = 0.4 m, U/U_{mf} = 1.5).

portion of a deep fluidized bed. Since the bubbles in a fluidized bed always move upward, the pressure fluctuations detected from the upper tap have a time delay compared to those detected from the lower tap; the delay time is equivalent to the traveling time of the bubbles from the lower tap to the upper tap. This is in agreement with the experimental results.

Figure 6 shows portions of two pressure fluctuation signals detected simultaneously in the lower portion of a deep fluidized bed, one at a position of 0.01 m above the distributor plate, and the other at a position of 0.12 m. A comparison of the two curves indicates that they are similar in shape, and the peaks and valleys of the two curves almost coincide. The cross-correlation function between these two pressure fluctuation signals confirms the fact that time shift was extremely small; it indicates that the pressure fluctuation signal at the position farther away from the distributor (0.12 m above the distributor) had a time advance of about 0.004 s over the position closer to the distribution (0.01 m above the distributor).

In the lower portion of the deep fluidized bed, it was generally observed that, when slugging occurred, the pressure fluctuation signal detected from the tap farther away from the distributor had a very small time advance compared to the signal detected from the tap closer to the distributor. However, when slugging did not occur (approximately $U/U_{mf} < 1.5$ for sand with $\overline{D}_p$ = 0.000711 m), this tendency was reversed, i.e., the pressure

TABLE 4. TIME SHIFT BETWEEN TWO PRESSURE FLUCTUATION SIGNALS DETECTED FROM TWO ADJACENT TAPS (L_s = 0.4 m, U/U_{mf} = 1.5).

Test Taps*	Time Shift (lower tap) (s)
1-2	−0.001
2-3	−0.001
3-4	−0.001
4-5	0.0085
5-6	0.0085
6-7	0.029

*Tap position: 1—0.01 m above the distributor; 2—0.055 m; 3—0.105 m; 4—0.150 m; 5—0.195 m; 6—0.230 m; 7—0.285 m.

fluctuation signal detected from the tap closer to the distributor had a small time advance compared to the signal from the tap farther away from the distributor. For most of the runs, the major frequency observed in the lower portion of the deep fluidized bed was essentially the same as that observed in the upper portion (Table 3). This indicates that both fluctuations are probably caused by the same source.

It appears that the formation of large bubbles through bubble coalescence in the middle portion of the bed, the formation of small bubbles near the distributor and the jet flow immediately above the distributor, all affect the pressure fluctuations in the lower portion of a deep fluidized bed. The major fluctuations are caused by the formation of large bubbles and are transmitted downward from the middle portion of the bed toward the lower portion of the bed. The small fluctuations, which are caused by the jet flow and the formation of small bubbles and are transmitted upward, are superimposed on the major fluctuations.

As mentioned in the preceding paragraphs, the pressure wave is transmitted upward and downward in the upper and lower portions, respectively, of a deep fluidized bed accompanied by slugging. An attempt was made to approximately locate the position where the change in the direction occurred. This was accomplished by computing the cross-correlation function according to Eq. 10 between two fluctuation signals taken from several pairs of adjacent taps along the column. The position where the time shift, τ, changed its sign was taken as the location where the change in the direction of the pressure wave propagation occurred. For a fluidized bed with particles of a mean diameter of 0.000711 m and a static bed height of 0.4 m, and operated at $U/U_{mf} = 1.5$, this position was approximately 0.15 m above the distributor (Table 4). When the air flow rate was increased, this position was lowered. This trend is in agreement with that observed by Kadlec (1962) under the assumption that slug was formed at this position.

For a fluidized bed with a relatively low static bed height of 0.12 m to 0.25 m, the pressure wave was propagated similarly to a deep fluidized bed. In the upper portion of the bed, the pressure fluctuation signal detected from a tap near the top of the bed always had a time delay compared to the signal detected from a tap below it. In the lower portion of the bed, pressure fluctuation signals taken from any two taps almost coincided. The similarity of the pressure fluctuation phenomena between the relatively shallow and deep fluidized beds indicates that the cause of pressure fluctuations in the two beds is very similar.

Pressure Fluctuations in the Bed

The trends in the changes in the amplitude, root mean square and 90% fluctuating interval of the pressure fluctuations are similar, Figure 15. For shallow fluidized beds, the results in Table 2 show that at the position 0.01 m above the distributor, the major frequency of pressure fluctuations decreased slightly with the air flow rate for the bigger particles and increased slightly for the smaller particles. However, the amplitude always increased with the air flow rate. For deep fluidized beds, the results in Table 3 show that the major frequency essentially remained invariant along the column at a fixed air flow rate and increased slightly or negligibly when the air flow rate was increased. The amplitude increased with the air flow rate at any given position. When the air flow rate was fixed, the amplitude of pressure fluctuations tended to increase and then decrease along the column height from the bottom to the top. The height where the maximum amplitude occurred decreased with an increase in the air flow rate.

The fact that the major frequency of pressure fluctuations remained essentially constant along the column implies that the pressure fluctuations in a fluidized bed can be attributed to the same cause as discussed in the previous section. The trend for the amplitude to increase with the air flow rate was expected since the bubble size became larger when air flow rate was increased. The amplitude's tendency to increase and then decrease with the distance above the distributor indicates that the bed density plays an important role in determining the amplitude of the pressure fluctuations in a fluidized bed. The position where the bed density begins to decrease descended the column with an increase in the air flow rate (Fan et al., 1962), and thus the position where the maximum amplitude occurred also descended the column, as can be observed in Table 3. Tables 2 and 3 also show that the diameter of the holes in the distributor had little effect on the major frequency; however, the use of the distributor with a smaller hole diameter resulted in smaller fluctuating amplitudes in both the plenum and the bed.

As can be seen in Figure 10, the static bed height significantly influenced the major frequency of pressure fluctuations. The figure shows that the major frequencies decreased as the static bed height increased and that the particle size did not significantly affect the major frequencies. The major frequencies predicted by Eq. 12 are also plotted in the figure. It appears that the predicted results are, at least, in qualitative or semiquantitative agreement with the experimental results. This indicates a need to develop a model which is capable of quantitatively describing the bed fluctuation phenomena.

The shapes of the probability density functions of the pressure fluctuations in a fluidized bed were different at different locations in the bed. Figure 11 shows that the density of a pressure fluctuation signal skews to the negative side of its mean at the bottom of the bed, skews to the positive side at the top of the bed and is almost symmetrical at the middle of the bed. The result observed at the bottom of the bed might be due to the fact that small fluctuations, which were caused by small bubbles, were superimposed on the major fluctuations, which were caused by the formation of large bubbles, in the lower half of the pressure-time curve. The superposition of the small fluctuations on the major fluctuations was almost always found in the lower half of the pressure-time curve, since the formation of small bubbles and thus the occurrence of small fluctuations were most likely to occur when the major fluctuations were at their valleys. The situation was reversed at the top of the bed, i.e., small fluctuations, possibly caused by the continuous raining of the sand, occurred at the upper half of the pressure fluctuations. As indicated in the figure, the kurtosis of the pressure fluctuations is essentially independent of the bed position.

A pressure vs. velocity plot in Figure 12 shows the changes in the mean pressure and the 90% fluctuating interval with the air flow rate at a position 0.15 m above the distributor. The particle size used was 0.000711 m and the static bed height was 0.40 m. The figure shows that the mean and the fluctuating interval increased with the air flow rate, and that the mean was not located at the center of the fluctuating interval when the air flow rate was high. This might be due to the low, relative position of the tap (0.15 m above the distributor) in the bed when the air flow rate was high.

ACKNOWLEDGMENT

The authors are grateful to the Department of Energy for financial support of this work under Grant ET-78-G-01-3376.

NOTATION

$\bar{D}_p$ = average particle diameter
D_t = bed diameter
L = bed height
L_s = static bed height
$f_{X(t)}$ = probability density function of $X(t)$
$F_{X(t)}$ = probability distribution function of $X(t)$
g = gravitational acceleration
K = kurtosis or flatness factor, Eq. 6
ΔP_{bed} = pressure drop across the bed
ΔP_d = pressure drop across the distributor
S = skewness factor, Eq. 5
S_{xx} = power spectral density function
T = duration of sampling

ΔT = time interval during which $X(t)$ locates itself between x and $x + \Delta x$, Eq. 1
U = superficial gas velocity
U_{mf} = superficial gas velocity at minimum fluidization
$X(t)$, $Y(t)$ = random variables

Greek Letters

μ = mean
μ_r = r-th central moment about the mean
σ = standard deviation
σ^2 = variance
τ = time shift variable, Eqs. 9 and 10
ϕ_{xx} = auto-correlation function of $X(t)$
ϕ_{xy} = cross-correlation function between $X(t)$ and $Y(t)$
ϵ = voidage of the bed
ϵ_{mf} = voidage at minimum fluidization
ω = angular frequency

LITERATURE CITED

Bendat, J. S., *Principles and Applications of Random Noise Theory*, John Wiley and Sons, Inc., New York (1958).
Brown, R. G., and J. W. Nilsson, *Introduction to Linear Systems Analysis*, John Wiley and Sons, Inc., New York (1962).
Crandall, S. H., and W. D. Mark, *Random Vibrations in Mechanical Systems*, Academic Press, New York (1963).
Davenport, J. B., and W. R. Root, *An Introduction to the Theory of Random Signals and Noise*, McGraw-Hill Book Co., Inc., New York (1958).
Fan, L. T., C. J. Lee, and R. C. Bailie, "Axial Solid Distribution in Gas-Solid Fluidized Beds," *AIChE J.*, **8**, 239 (1962).
Fiocco, R. J., Sc. D. Thesis, Stevens Institute of Technology, Hoboken, N. J. (1964).
Hiby, J. W., *Proceedings of the International Symposium of Fluidization, Eindhoven*, Netherlands Univ. Press, Amsterdam, p. 99 (1967).
Kadlec, R., "The Behavior of Slugging Gas-Fluidized Solids," Ph.D. Dissertation, University of Michigan (1962).
Kang, W. K., J. P. Sutherland, and G. L. Osberg, "Pressure Fluctuations in a Fluidized Bed with and without Screen Cylindrical Packings," *I&EC Fundamentals*, **6**, 449 (1967).
Lee, Y. W., *Statistical Theory of Communication*, John Wiley and Sons, Inc., New York (1960).
Lirag, R., and H. Littman, *Statistical Study of the Pressure Fluctuations in a Fluidized Bed*, AIChE Symp. Ser., **67**(116), 11 (1971).
Littman, H., and G. A. Homolka, "Bubble Rise Velocities in Two-Dimensional Gas-Fluidized Bed from Pressure Measurements," *Chem. Eng. Prog.*, **66** (105), 37 (1970).
Shuster, W. W., and P. Kisliak, "The Measurement of Fluidization Quality," *Chem. Eng. Prog.*, **48**, 455 (1952).
Sutherland, K. S., Argonne National Laboratory, Rept. ANL-6907 (1964).
Swinehart, F. M., "A Statistical Study of Local Wall Pressure Fluctuations in Gas Fluidized Columns," Ph.D. Dissertation, University of Michigan (1966).
Tamarin, A. I., "The Origin of Self-Excited Oscillations in Fluidized Beds," *Int. Chem. Eng.*, **4**, 50 (1964).
Verloop, J., and P. M. Heertjes, "Periodic Pressure Fluctuations in Fluidized Beds," *Chem. Eng. Sci.*, **29**, 1035 (1974).
Winter, O., Density and Pressure Fluctuations in Gas Fluidized Beds," *AIChE J.*, **14**, 426 (1968).
Wong, H. W., and M. H. I. Baird, "Fluidization in a Pulsed Gas Flow," *Chem. Eng. J.*, **2**, 104 (1971).

Manuscript received September 14, 1979; revision received July 21, and accepted July 25, 1980.

Bacterial Film Growth in Adsorbent Surfaces

G. F. ANDREWS
and
CHI TIEN

Department of Chemical Engineering and Materials Science
Syracuse University
Syracuse, NY 13210

Simultaneous biological and activated-carbon treatment of organic wastewaters appears promising. The effects of bacterial film growth on adsorbent particles is investigated by laboratory work and mathematical modelling. Regeneration of the adsorbent due to film growth does occur, but faster than predicted. The discrepancy reflects uncertainty about the structure of bacterial films.

SCOPE

A promising method for removing soluble organic matter from wastewater is to combine biological treatment and activated carbon adsorption into a single unit. This is demonstrated by the PACT system (addition of powdered carbon to an activated sludge unit), the effects of bacterial growth in carbon adsorption columns, and various proposals for the biological regeneration of spent carbon.

This paper provides a mathematical model on which the design and evaluation of such systems can be based. It predicts the uptake rates of organic matter due to adsorption and biological activity when a bacterial film grows on a granular carbon particle. The predictions are compared with experimental data from a laboratory-scale, fluidized-bed reactor operated with a high-recirculation rate. The organic substrate is valeric acid, and denitrifying bacteria are used.

Unlike previous work, this model is applicable to films which are actively growing and are thick enough to cause bioregeneration. Also, all theoretical and practical work is done in a way that could be repeated on a real wastewater whose constituents are dilute, soluble, biodegradable, and adsorbable. Procedures are given for the measurement of all but one of the model's parameters. The bacterial growth rate and yield values are determined from experiments with beds of nonadsorbing coal particles.

G. F. Andrews is presently with the Department of Chemical Engineering, State University of New York at Buffalo, Buffalo, NY 14262.